BIOCHEMISTRY
including biophysical chemistry & molecular biology

Article

pubs.acs.org/biochemistry

S-Nitrosation Destabilizes Glutathione Transferase P1-1

David Balchin,[†] Stoyan H. Stoychev,[‡] and Heini W. Dirr*[,†]

[†]Protein Structure-Function Research Unit, School of Molecular and Cell Biology, University of the Witwatersrand, Johannesburg, South Africa

[‡]CSIR Biosciences, Pretoria, South Africa

Supporting Information

ABSTRACT: Protein *S*-nitrosation is a post-translational modification that regulates the function of more than 500 human proteins. Despite its apparent physiological significance, *S*-nitrosation is poorly understood at a molecular level. Here, we investigated the effect of *S*-nitrosation on the activity, structure, stability, and dynamics of human glutathione transferase P1-1 (GSTP1-1), an important detoxification enzyme ubiquitous in aerobes. *S*-Nitrosation at Cys47 and Cys101 reduces the activity of the enzyme by 94%. Circular dichroism spectroscopy, acrylamide quenching, and amide hydrogen−deuterium exchange mass spectrometry experiments indicate that the loss of activity is caused by the introduction of local disorder at the active site of GSTP1-1. Furthermore, the modification destabilizes domain 1 of GSTP1-1 against denaturation, smoothing the unfolding energy landscape of the protein and introducing a refolding defect. In contrast, *S*-nitrosation at Cys101 alone introduces a refolding defect in domain 1 but compensates by stabilizing the domain kinetically. These data elucidate the physical basis for the regulation of GSTP1-1 by *S*-nitrosation and provide general insight into the consequences of *S*-nitrosation on protein stability and dynamics.

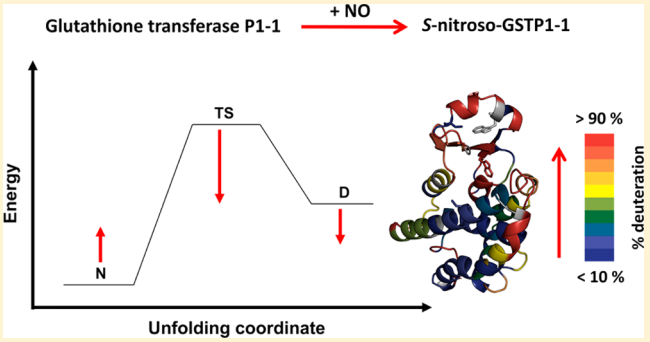

S-Nitrosation is a post-translational modification of cysteine residues in proteins that results from the formation of a covalent complex between NO and the cysteine thiol. Increasingly intensive study is confirming the importance of this modification alongside other, more extensively studied post-translational modifications such as phosphorylation, glycosylation, and ubiquitination. *S*-Nitrosation affects a wide range of proteins,[1] regulates a number of physiological phenomena,[2,3] and has been linked to several diseases.[4]

S-Nitrosation has been shown to induce enzyme activation[5] or inhibition[6] and to regulate the activity of several ion channels[7,8] and control the allosteric behavior of hemoglobin.[9] Despite the clear importance of *S*-nitrosation to the physiological regulation of protein function, relatively little is known about the molecular origins of these effects. Specifically, biophysical data linking the *S*-nitrosation event to its functional consequence are lacking. Far-UV circular dichroism spectroscopy revealed a small loss of α-helical content upon *S*-nitrosation of OxyR[10] and the chloride channel CLIC4,[11] and a subtle change in the tertiary structure of *S*-nitrosated CLIC4 was suggested by trypsin digestion and thermal denaturation experiments.[11] *S*-Nitrosation has also been shown to regulate the immune response in plants by triggering the oligomerization of NPR1.[12] Only four crystal structures and two solution structures [nuclear magnetic resonance (NMR)] have been determined for *S*-nitrosated proteins to date: myoglobin,[13] thioredoxin,[14] protein-tyrosine phosphatase 1B,[15] nitrophorin,[16] p21^{Ras17} (NMR), and S100A1[18] (NMR). The limited size of this structural data set makes it difficult to identify trends or make predictions about the consequences of *S*-nitrosation on protein structure. In addition, structural data need to be linked to changes in protein function, stability, and dynamics to completely elucidate *S*-nitrosation at a molecular level.

In this study, we explore the effect of *S*-nitrosation on the activity, structure, stability, and dynamics of human glutathione transferase P1-1 (GSTP1-1). GSTP1-1 is a homodimeric detoxification enzyme that solubilizes toxins by conjugation to glutathione and regulates cell proliferation by inhibition of c-jun N-terminal kinase. *S*-Nitrosated GSTP1-1 is known to exist *in vivo*,[19−21] and *in vitro* work has demonstrated that the modification affects the detoxification activity of the enzyme.[22] Given that the target cysteines are not directly involved in catalysis by GSTP1-1, it is not clear how the *S*-nitrosation event causes the apparent loss of activity. Here, we provide experimental evidence of a severe disruption of GSTP1-1 stability and domain 1 dynamics upon *S*-nitrosation at Cys47 and Cys101. These data detail the regulation of GSTP1-1 by *S*-nitrosation and provide insight into the biophysical basis for protein regulation by *S*-nitrosation in general.

Received: October 16, 2013
Revised: November 22, 2013
Published: November 22, 2013

   dx.doi.org/10.1021/bi401414c | *Biochemistry* 2013, 52, 9394−9402

EXPERIMENTAL PROCEDURES

Protein Expression, Purification, and *S*-Nitrosation. The pET-15b vector encoding N-terminally His_6-tagged GSTP1-1 was a kind gift from S. Y. Blond (Centre for Pharmaceutical Biotechnology, University of Illinois, Chicago, IL). His_6-GSTP1-1 was expressed in *Escherichia coli* T7 cells and purified by Co^{2+} affinity chromatography as described previously.[23] *S*-Nitrosated GSTP1-1 was prepared by mixing fully reduced protein (with or without a 50-fold molar excess of glutathione sulfonate) with a 50-fold molar excess of *S*-nitrosoglutathione (GSNO) at 37 °C for 1 h. Excess GSNO was removed by dialysis or buffer exchange. The *S*-nitrosation stoichiometry was determined by UV difference spectroscopy as described previously[22] based on an S-NO extinction coefficient of 750 M^{-1} cm^{-1} at 330 nm.

Steady-State Enzyme Kinetics. Enzyme activity was measured at 20 °C for the conjugation of GSH to CDNB.[24] GSH (1 mM) and CDNB (1 mM) were mixed with 1−10 nM enzyme in 100 mM sodium phosphate buffer (pH 6.5) with 1 mM EDTA, 0.02% sodium azide, and 3% (v/v) ethanol. Product formation was monitored by the absorbance at 340 nm. All measurements were performed in triplicate and corrected for the nonenzymatic reaction rate.

Steady-State Spectroscopic Measurements. Fluorescence emission spectra were recorded using a Jasco FP-6300 fluorescence spectrophotometer. Excitation was at 280 nm, and protein concentrations were 2 μM in 20 mM phosphate buffer (pH 7.4) with 150 mM NaCl, 2 mM EDTA, and 0.02% sodium azide. For the acrylamide quenching experiments, excitation was at 295 nm and emission was collected at 342 nm. The protein concentration was 1 μM, and the acrylamide concentration was varied between 0 and 0.3 M. For denatured-state quenching, the protein was equilibrated in 8 M urea before the fluorescence measurements, and *N*-acetyltryptophanamide was included as a control. The quenching data were fit to a modified form of the Stern−Volmer equation (Lehrer plot), for systems with multiple fluorophores:[25,26]#tab;

$$\frac{F_0}{F_0 - F} = \frac{1}{f_a K_Q [Q]} + \frac{1}{f_a}$$

where F_0 is the total fluorescence in the absence of a quencher (contributed by both the accessible and nonaccessible fractions of fluorophores), F is the fluorescence at a particular quencher concentration, K_Q is the Stern−Volmer quenching constant of the accessible fraction, [Q] is the concentration of quencher (acrylamide), and f_a is the fraction of the initial fluorescence accessible to the quencher.

Far-UV circular dichroism measurements were performed in triplicate on a Jasco J810 circular dichroism spectropolarimeter with 2 μM protein in the same buffer as the fluorescence measurements. The raw data were averaged and converted to mean residue ellipticity, $[\theta]$ (degrees square centimeters per decimole) using the following equation:#tab;

$$[\theta] = \frac{100\theta}{Cnl}$$

where θ is the measured ellipticity (millidegrees), C is the protein concentration (millimolar), n is the number of residues, and l is the path length (centimeters).

Equilibrium Unfolding and Refolding. Equilibrium unfolding experiments were conducted by mixing 1 μM protein [20 mM phosphate buffer (pH 7.4) with 150 mM NaCl, 2 mM EDTA, and 0.02% sodium azide] with 0−8 M urea. Refolding was initiated by diluting 10 μM protein in 8 M urea into 1−7.8 M urea with a final protein concentration of 1 μM. All solutions were prepared in triplicate and allowed to equilibrate for 30 min before the structure of the proteins was probed using fluorescence spectroscopy (λ_{ex} = 280 nm; λ_{em} = 342 nm) and circular dichroism at 222 nm.

Unfolding Kinetics. Unfolding kinetics were measured by intrinsic fluorescence using a stopped-flow instrument (Applied Photophysics SX-18MV). Excitation was at 280 nm, and emission was collected using a 320 nm long-pass filter. Final protein concentrations were 1 μM, and the urea concentration was varied from 5.5 to 8 M in 20 mM phosphate buffer (pH 7.4) with 150 mM NaCl, 2 mM EDTA, and 0.02% sodium azide. At least three traces were recorded and averaged at each urea concentration, and the data were fit to single- or double-exponential equations in SigmaPlot version 11.0. The dependence of the observed rate constants on urea concentration was fit to the following equation:

$$\log k_u = \log k_u^{H_2O} + \frac{m_u^{\ddagger}[\text{urea}]}{2.303RT}$$

where k_u is the observed unfolding rate constant, $k_u^{H_2O}$ is the unfolding rate constant in the absence of urea, and $m_u^{\ddagger}$ is the m value for the unfolding of the native state to form the transition state.

Hydrogen−Deuterium Exchange Mass Spectrometry. For the on-exchange reactions, 10 μL of reduced or *S*-nitrosated GSTP1-1 at a concentration of 8 mg/mL [20 mM phosphate buffer (pH 7.4) with 150 mM NaCl, 2 mM EDTA, and 0.02% sodium azide] was diluted with 40 μL of 100% D_2O at 20 °C for 10, 15, 30, 100, 300, or 3600 s before the simultaneous quench, reduction, and proteolysis as previously described.[27] Ice-cold quench buffer was added in an equal volume to the reaction buffer and contained 1 mg/mL pepsin (Sigma), 100 mM TCEP, and 2 M guanidinium chloride. For the fully deuterated control, deuteration was conducted overnight and the buffer was supplemented with 0.02% formic acid. The nondeuterated control experiment was performed as described above except MilliQ H_2O was used in place of D_2O. Following addition of the quench buffer, proteolysis was allowed to proceed for 5 min before the samples were injected onto an Aeris PEPTIDE 3.6 μm XB-C18 RP column (Phenomenex), submerged in ice, coupled to an AB SCIEX QSTAR Elite mass spectrometer via a six-port switching valve. Peptides were eluted at a rate of 300 μL/min with a linear acetonitrile gradient (5 to 95%) over 15 min. Initial peptide identification was performed using collision-induced dissociation (CID) in information-dependent acquisition (IDA) mode, and all subsequent samples were analyzed in MS mode. All reactions were performed in duplicate. The initial peptide pool was sequenced using PEAKS 6 (Bioinformatics Solutions Inc.), and deuterium exchange data were processed using HDExaminer 1.3 (Sierra Analytics).

RESULTS

***S*-Nitrosation of GSTP1-1 *in Vitro*.** GSTP1-1 *S*-nitrosated at Cys47 and Cys101 exists *in vivo*[19−21] and has previously been generated *in vitro*.[22,28] Here, we produced *S*-nitrosated GSTP1-1 by reaction with GSNO, the most prominent physiological transnitrosation agent.[29] *S*-Nitrosation was confirmed by ESI-

dx.doi.org/10.1021/bi401414c | *Biochemistry* 2013, 52, 9394−9402

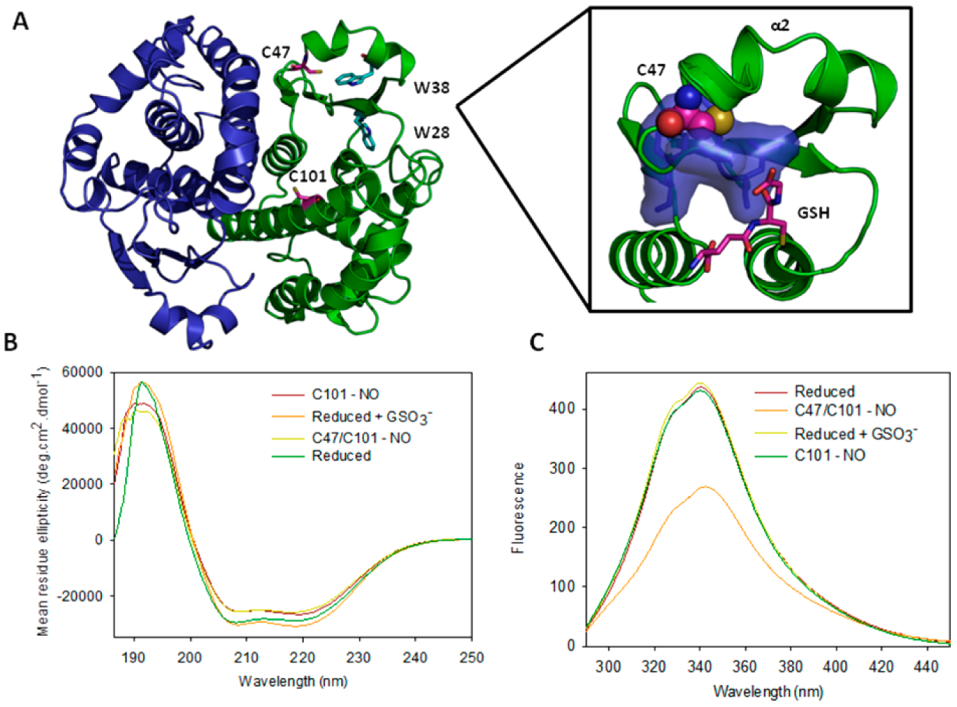

Figure 1. *S*-Nitrosation does not substantially alter the structure of GSTP1-1. (A) Dimeric human GSTP1-1 (PDB entry 6GSS). The sites of nitrosation, Cys47 and Cys101, are indicated (magenta), as are the locations of Trp28 and Trp38, the two tryptophan residues in each subunit (cyan). The inset shows the active site of GSTP1-1 showing the glutathione binding site and packing of Cys47. Glutathione (GSH, magenta sticks) does not interact directly with Cys47 of the protein, nor does the cysteine thiol participate in catalysis. Packing of Cys47 into a hydrophobic pocket (blue surface) maintains the conformation of helix α2 and the GSH binding site. (B) Circular dichroism spectra for reduced and *S*-nitrosated GSTP1-1. The raw data were converted to mean residue ellipticity (MRE) as described in Experimental Procedures. (C) Fluorescence spectra of reduced and *S*-nitrosated GSTP1-1 with a λ_{ex} of 280 nm.

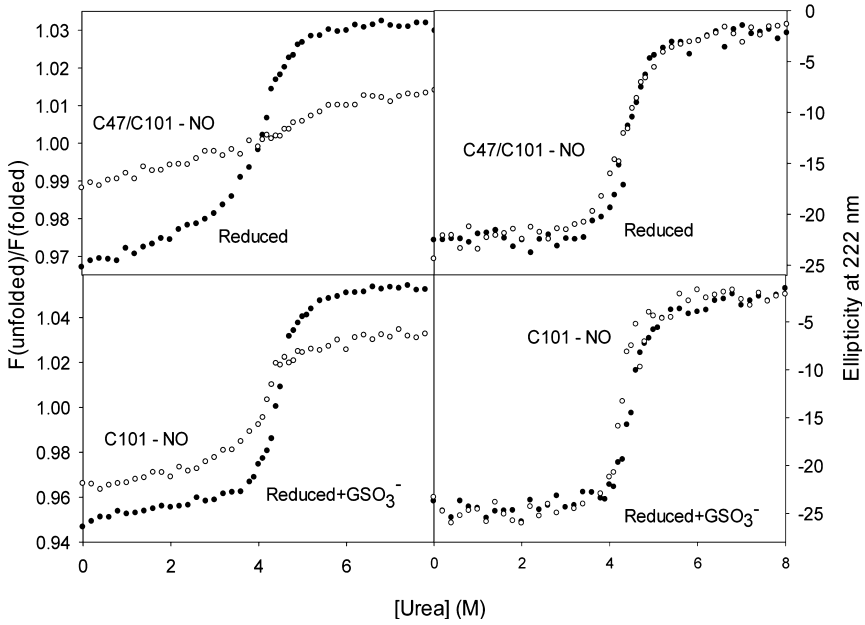

Figure 2. *S*-Nitrosation reduces the unfolding cooperativity in domain 1 of GSTP1-1. Urea-induced unfolding of reduced GSTP1-1 (●) and *S*-nitrosated variants (○) monitored by tryptophan fluorescence with a λ_{ex} of 280 nm (A and C) and circular dichroism at 222 nm (B and D). Data points are the average of three replicates.

MS,[30] and the stoichiometry of nitrosation was determined by UV absorption to be 2 ± 0.1 *S*-nitrosothiols per subunit, consistent with previous reports. Cys101 of GSTP1-1 has been identified as an unusually long-lived *S*-nitrosocysteine *in vivo*.[19] We produced GSTP1-1 Cys101-NO by saturating the protein with glutathione sulfonate (GSO_3^-) before reaction with GSNO. GSO_3^- binds the active site and prevents Cys47 nitrosation by inducing the closed state of α2,[30] resulting in an *S*-nitrosation stoichiometry of 1.2 ± 0.1 per subunit. In all subsequent experiments, GSTP1-1 Cys101-NO was compared

dx.doi.org/10.1021/bi401414c | *Biochemistry* 2013, 52, 9394−9402

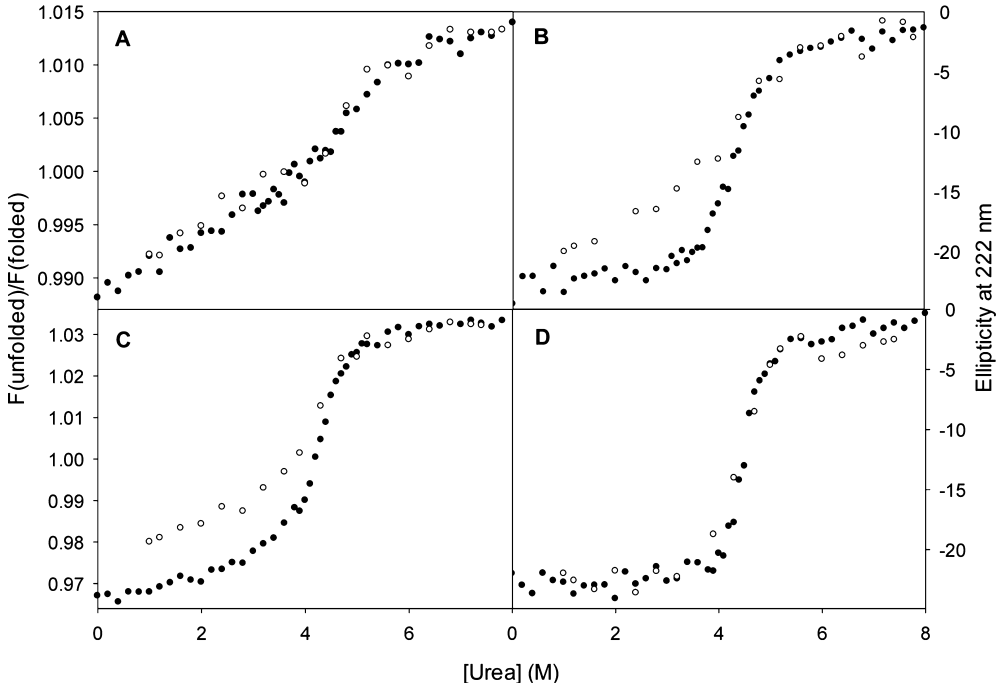

Figure 3. *S*-Nitrosation of GSTP1-1 introduces a refolding defect. Urea-induced unfolding (●) and refolding (○) of GSTP1-1 and *S*-nitrosated variants monitored by tryptophan fluorescence with a λ_{ex} of 280 nm (A and C) and circular dichroism at 222 nm (B and D). (A and B) Cys47/Cys101-NO and (C and D) Cys101-NO. Data points are the average of three replicates.

to reduced GSTP1-1 saturated with GSO_3^-, to control for the presence of the ligand.

***S*-Nitrosation Severely Impairs the Enzyme Activity but Does Not Substantially Alter the Structure of GSTP1-1.** GSTP1-1 catalyzes the conjugation of reduced glutathione to a variety of drugs and toxins, including several chemotherapeutic agents. Although neither Cys47 nor Cys101 is directly involved in catalysis, Cys47 is thought to contribute to maintaining the conformation of the active site by interacting with a hydrophobic pocket in domain 1 (Figure 1A) and, in the thiolate form, with Lys54.[31] Cys101 is highly solvent-exposed, and the Cys101 thiol does not appear to make any stabilizing interactions with the rest of the protein. The enzyme activity of reduced and *S*-nitrosated GSTP1-1 was evaluated using the standard CDNB/GSH conjugation assay.[24] *S*-Nitrosation at Cys47 and Cys101 caused a 94% decrease in the specific activity of the enzyme, from 96 μmol min^{-1} mg^{-1} (reduced) to 6 μmol min^{-1} mg^{-1} (Cys47/Cys101-NO).

We used several spectroscopic methods to probe the effect of *S*-nitrosation on the structure of GSTP1-1 in solution. Circular dichroism spectra are similar for reduced and *S*-nitrosated GSTP1-1, although a small decrease in the level of α-helical structure is apparent for the Cys47/Cys101-NO and Cys101-NO proteins (Figure 1B). Steady-state fluorescence (λ_{ex} = 280 nm) shows substantial quenching of tryptophan fluorescence for Cys47/Cys101-NO GSTP1-1 (Figure 1C). This quenching effect is most likely due to Förster resonance energy transfer between the two tryptophan residues in each subunit (Trp28 and Trp38) and Cys47-NO (Figure 1A)[32] and does not necessarily indicate a structural change in the vicinity of the tryptophans. In support of this interpretation, no significant shift in the maximal emission wavelength is apparent. Acrylamide quenching was used to compare the accessibility of tryptophan residues in reduced and *S*-nitrosated GSTP1-1. Within error, the effective quenching constants (K_Q) for reduced (1.7 ± 0.4 M^{-1}) and Cys101-NO (1.8 ± 0.5 M^{-1}) GSTP1-1 are identical, and very similar to that reported previously.[33,34] The K_Q for quenching of Cys47/Cys101-NO GSTP1-1 (2.8 ± 0.3 M^{-1}) is slightly elevated, however, suggesting that one or both tryptophans are more solvent-exposed in the *S*-nitrosated protein.

***S*-Nitrosation Reduces the Unfolding Cooperativity in Domain 1 of GSTP1-1.** To investigate the effect of *S*-nitrosation on the stability of GSTP1-1, we monitored the unfolding equilibrium of the protein using circular dichroism and fluorescence spectroscopy (Figure 2). The majority of the helical structure of GSTP1-1 is located in domain 2, while both tryptophan residues are in domain 1 (Figure 1A). CD ellipticity at 222 nm is therefore primarily a probe of domain 2 unfolding, while tryptophan fluorescence reports on the unfolding of domain 1.[35] Neither *S*-nitrosation at Cys47 and Cys101 nor *S*-nitrosation at Cys101 alone affects the unfolding of domain 2 of GSTP1-1 (ellipticity at 222 nm) (Figure 2B,D). *S*-Nitrosation does, however, significantly influence the unfolding equilibrium of domain 1. While the unfolding of the reduced protein shows a sigmoidal, cooperative transition, the profile for Cys47/Cys101 nitrosated GSTP1-1 is almost linear (Figure 2A). The dependence of unfolding on denaturant concentration (*m* value) is therefore significantly decreased. This implies that *S*-nitrosation at both cysteines severely impairs the cooperativity of unfolding of domain 1 and reduces the change in solvent accessible surface area upon unfolding.[36] In addition, the starting point of the unfolding curve is higher for the modified protein, but the denaturation end point is lower than that for reduced GSTP1-1. *S*-Nitrosation of GSTP1-1 may therefore result in a partially unfolded "native" state that fails to unfold to the same degree as the reduced protein, even at high denaturant concentrations. This observation is supported by acrylamide quenching experiments in 8 M urea. While the tryptophans of reduced GSTP1-1 in the denatured state are completely

dx.doi.org/10.1021/bi401414c | *Biochemistry* 2013, 52, 9394−9402

accessible to quencher, the Lehrer plot for the *S*-nitrosated protein indicates that 34% of its tryptophan fluorescence is inaccessible to quenching by acrylamide. The denatured state of *S*-nitrosated GSTP1-1 is therefore unusually compact.

Similar to double nitrosation at Cys47 and Cys101, Cys101 nitrosation results in a less cooperative unfolding transition for domain 1 of GSTP1-1 (Figure 2C). In addition, the starting and ending points of the curve suggest that the modified protein is partially unfolded initially but retains more "folded" character than the unmodified protein when denaturation is complete. This effect is much less pronounced, however, than for Cys47/Cys101-NO GSTP1-1.

Because of refolding hysteresis (discussed below), the unfolding transitions in Figure 2 could not be fit to a model for equilibrium unfolding.

S-Nitrosation Causes a Refolding Defect in GSTP1-1. We examined the refolding equilibrium of reduced and *S*-nitrosated GSTP1-1 using circular dichroism and fluorescence spectroscopy (Figure 3). Unlike the reduced protein, which unfolds and refolds reversibly (not shown), *S*-nitrosated GSTP1-1 refolds defectively. Domain 1 of Cys47/Cys101-NO GSTP1-1 (monitored by fluorescence) refolds reversibly (Figure 3A). Circular dichroism measurements, however, reveal hysteresis in domain 2 refolding (Figure 3B). The shallow slope of the refolding transition suggests that domain 2 folds less cooperatively than it unfolds and implies a smaller change in solvent accessible surface area upon folding.[36] Despite the hysteresis, the native state is essentially completely recovered at low urea concentrations.

While circular dichroism measurements suggest that the α-helical structure of Cys101-NO GSTP1-1 is completely and reversibly recovered upon dilution of the denaturant (Figure 3D), folding hysteresis is detected by tryptophan fluorescence (Figure 3C). The hysteresis is apparent from approximately 4 M urea (the midpoint of the unfolding transition), with the folding transition displaying a slope that is shallower than that for unfolding. In addition, the fluorescence signal, and therefore the structure of domain 1, is not completely recovered at low urea concentrations. Light scattering data (not shown) suggest that the hysteresis and lack of recovery of the native state are not the result of protein aggregation.

S-Nitrosation Alters the Unfolding Pathway of GSTP1-1. Equilibrium unfolding experiments demonstrate that *S*-nitrosation severely destabilizes domain 1 of GSTP1-1. To further understand the effect of *S*-nitrosation on the unfolding of the protein, we measured unfolding kinetics using a stopped-flow instrument (Figure 4). Structural changes were followed by intrinsic fluorescence, thereby focusing on the local environment of Trp28 and Trp38 in domain 1 (Figure 1A).

The unfolding of the reduced protein shows two phases: a positive amplitude burst phase followed by a negative amplitude phase (Figure 4A). The positive amplitude phase has previously been attributed to the unfolding of helix 2.[35] This burst phase is largely unresolved, with approximately 1% of the signal captured, and was therefore excluded from the fit. In contrast, the negative amplitude phase is well-defined and was fit to a single-exponential decay function. The unfolding of reduced GSTP1-1 in complex with GSO_3^- follows kinetics very similar to those of the apoenzyme.

The *S*-nitrosated isoforms of GSTP1-1 show unfolding kinetics substantially different from those of the reduced proteins (Figure 4A). In contrast to the positive amplitude burst phase and negative amplitude slow phase of the reduced

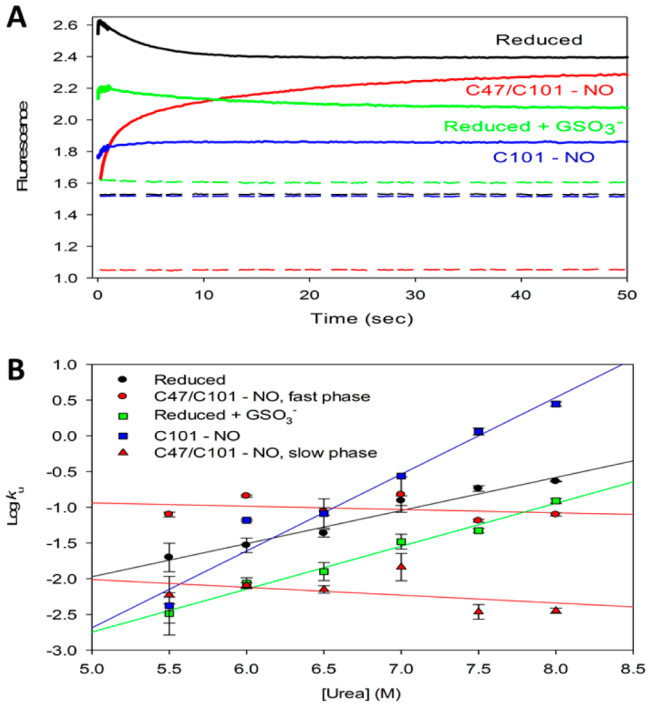

Figure 4. *S*-Nitrosation alters the unfolding pathway of GSTP1-1. (A) Fluorescence transients after mixing 1 μM reduced or *S*-nitrosated GSTP1-1 with 8 M urea: reduced (black), Cys47/Cys101-NO (red), reduced with GSO_3^- (green), and Cys101-NO (blue). Fluorescence transients for the protein mixed with buffer only are shown with dashed lines. λ_{ex} = 280 nm, and λ_{em} = 342 nm. For the reduced proteins (apo and liganded), the first phase (rapid increase in fluorescence) occurred too rapidly to be well resolved and only the second phase (slow decrease in fluorescence) was fit to a single-exponential decay function. The unfolding transient for Cys47/Cys101-NO was fit to a double-exponential function, while the transient for Cys101-NO fit well to a single-exponential function. (B) Urea dependence of the observed unfolding rate constants for the proteins in panel A. The data were fit to a linear function as described in Experimental Procedures, and the fit parameters are listed in Table 1. Data points are the average of three replicates, and error bars represent the standard deviation.

proteins, both Cys47/Cys101-NO and Cys101-NO GSTP1-1 show only positive amplitude phases. These events occur on a time scale much longer than that of the burst phase for the reduced proteins, and only a small proportion of the signal is not captured. While the unfolding of Cys101-NO GSTP1-1 fits well to a single-exponential function, the unfolding kinetics of Cys47/Cys101-NO GSTP1-1 are better described by a double-exponential function.

To characterize the unfolding kinetics further, the rate constants for the resolvable phases of unfolding were determined as a function of urea concentration (Figure 4B). Because the *S*-nitrosated and reduced proteins do not appear to follow the same unfolding pathway (Figure 4A), the constants reported in Table 1 are not necessarily for the same structural events and therefore cannot be directly compared. The data are nonetheless informative with regard to the character of the individual phases. For the reduced proteins, GSO_3^- binding does not significantly alter the kinetic cooperativity (m value). However, the ligand does appear to stabilize the native state of domain 1 of the reduced protein, which is evident in the 25-fold decrease in $k_u^{H_2O}$, consistent with previous work.[35] The unfolding of Cys101-NO GSTP1-1 is monophasic and different

dx.doi.org/10.1021/bi401414c | *Biochemistry* 2013, 52, 9394−9402

Table 1. Kinetic Constants for the Unfolding of Reduced and *S*-Nitrosated GSTP1-1

	reduced	reduced with GSO_3^-	Cys101-NO (with GSO_3^-)	Cys47/Cys101-NO, fast phase	Cys47/Cys101-NO, slow phase
$k_u^{H_2O}$ (s^{-1})	$(5 \pm 2) \times 10^{-5}$	$1.8 \times 10^{-6} \pm 6 \times 10^{-7}$	$(3 \pm 2) \times 10^{-8}$	0.21 ± 0.11	0.04 ± 0.02
$m_u^{\ddagger}$ (kcal mol^{-1} M^{-1})	0.62 ± 0.04	0.81 ± 0.04	1.3 ± 0.1	-0.07 ± 0.06	-0.06 ± 0.08

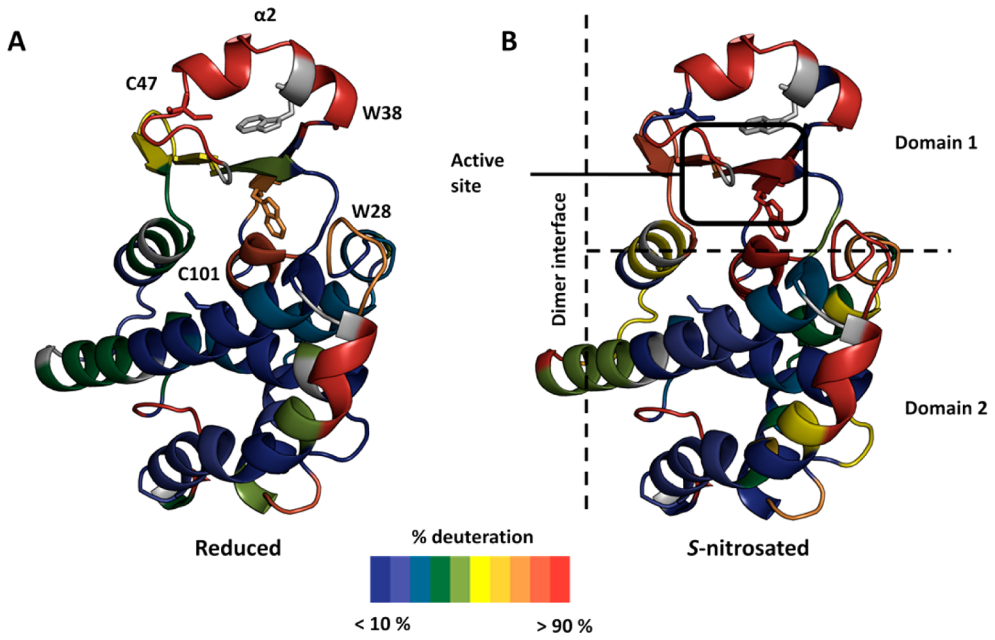

Figure 5. Conformational dynamics of reduced and *S*-nitrosated GSTP1-1 probed by DXMS. The percentages of deuteration of (A) reduced and (B) *S*-nitrosated GSTP1-1 after 100 s are mapped onto the structure of a single subunit of the protein (PDB entry 6GSS). The highly dynamic α2 helix is indicated, as are the *S*-nitrosation target cysteines (C47 and C101) and the dominant fluorophores (W28 and W38).

from that of the reduced proteins. The large $m_u^{\ddagger}$ and small $k_u^{H_2O}$ indicate that this phase represents the highly cooperative unfolding of a stable structural element in domain 1. The two phases (fast and slow) in the unfolding of Cys47/Cys101-NO GSTP1-1 are both characterized by a very low $m_u^{\ddagger}$ and a high $k_u^{H_2O}$. In contrast to Cys101-NO GSTP1-1, this suggests the unfolding of an unstable structural element that experiences a small change in solvent accessible surface area between the native and transition states.

S-Nitrosation Increases the Conformational Dynamics of GSTP1-1. To rationalize the effect of *S*-nitrosation on the stability and activity of GSTP1-1, the dynamics of the reduced and modified proteins were probed using amide hydrogen−deuterium exchange mass spectrometry (DXMS) (Figure 5). In both reduced and *S*-nitrosated GSTP1-1, α2 rapidly exchanges nearly all of its amide protons. This is consistent with NMR data that showed that α2 is largely disordered above 17 °C[37] and therefore poorly protected from deuterium exchange. In contrast, the helical bundle comprising domain 2 is relatively stable in both proteins, in agreement with DXMS data for class mu GSTM1-1[38] and the GST homologue CLIC1.[39]

The deuteration difference map and peptide deuteration kinetics reveal substantial differences in amide hydrogen exchange behavior between reduced and *S*-nitrosated GSTP1-1 (Figure 6 and Figures S1 and S2 of the Supporting Information). Although α2 is equally susceptible to deuteration in both proteins, the rest of domain 1 is significantly more dynamic in *S*-nitrosated GSTP1-1. Specifically, strands β1−β3, helices α1 and α3, and the apex of helix α8 all show higher levels of deuteration in the modified protein over 10−3600 s. The exception to this trend is part of the peptide that includes *S*-nitrosated Cys47 (residues 37−47), which exchanges fewer deuterons than in the reduced protein, suggesting that this region is locally protected from deuterium exchange. The dynamics of domain 2 are also affected by *S*-nitrosation, particularly over longer time scales (>30 s), evident in the increased level of deuteration of α4, α5, and α7. Together, the DXMS data show that *S*-nitrosation at Cys47 and Cys101 destabilizes both domain 1 and domain 2 of GSTP1-1.

DISCUSSION

S-Nitrosation is a post-translational modification with a wide range of substrates and clear physiological relevance. Despite this, the molecular mechanisms by which this cysteine modification effects changes in protein function remain poorly understood. Here, we investigated the effect of *S*-nitrosation on the activity, stability, structure, and dynamics of GSTP1-1, with the aim of understanding how the activity of this ubiquitous enzyme is regulated. We found that *S*-nitrosation destabilizes GSTP1-1, causing domain 1 of the protein to unfold with low cooperativity and introducing a global refolding defect.

S-Nitrosation was previously observed to reduce the activity of GSTP1-1 *in vitro* by 30%.[22] We observed a substantially larger reduction in activity (94%), possibly due to the fact that we nitrosated the protein at 37 °C instead of 25 °C, resulting in a larger proportion of the population of the protein being modified.[30] Despite the significant decrease in enzyme activity, our spectroscopic analyses revealed little structural difference between the *S*-nitrosated and reduced isoforms, except for a small reduction in α-helical content and a change in acrylamide

dx.doi.org/10.1021/bi401414c | *Biochemistry* 2013, 52, 9394−9402

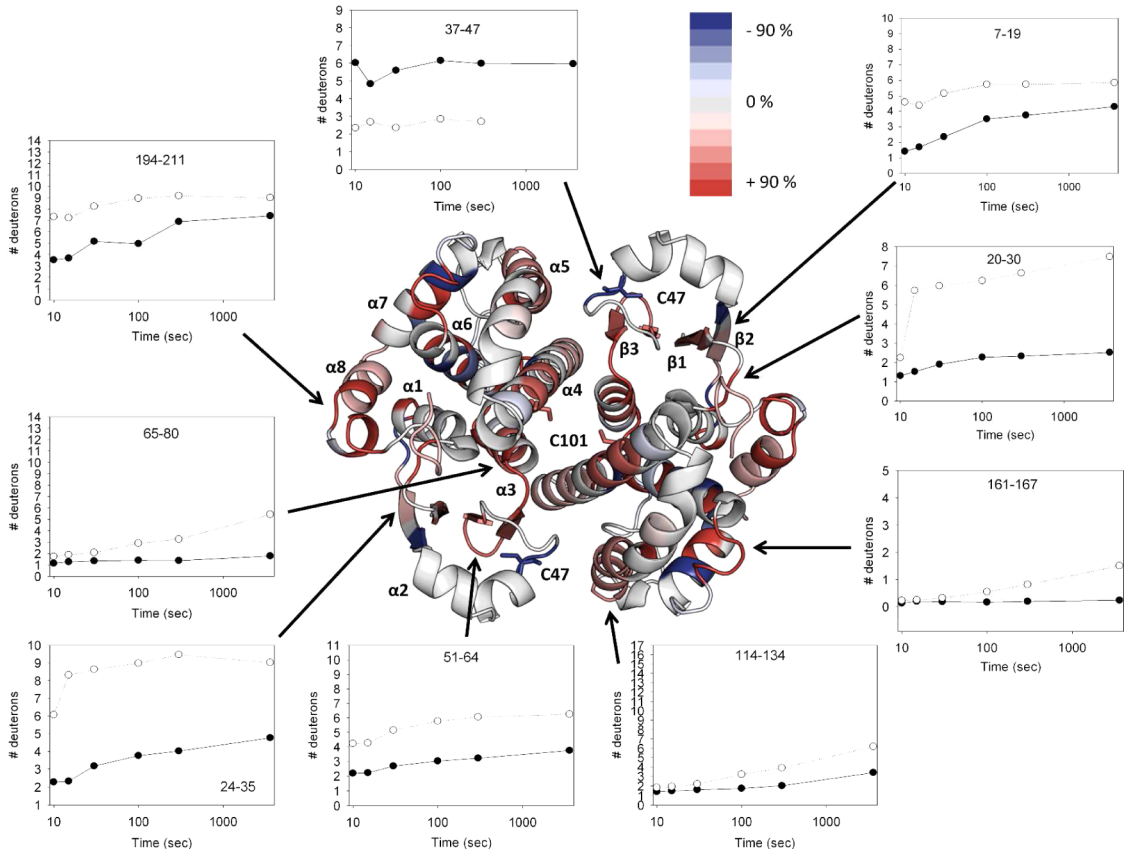

Figure 6. *S*-Nitrosation increases the conformational flexibility of GSTP1-1. The percentage differences in deuteration between reduced and *S*-nitrosated GSTP1-1 after 100 s are mapped onto the structure of dimeric GSTP1-1 (PDB entry 6GSS), calculated as the percentage of deuteration (*S*-nitrosated) minus the percentage of deuteration (reduced). Red coloring indicates that the level of deuterium exchange is higher for the nitrosated protein, while blue coloring indicates that the level of deuterium exchange is higher for the reduced protein. Helices α1−α8 are labeled, and the target cysteines (Cys47 and Cys101) are shown as sticks. The deuteron uptake plots compare deuteron incorporation of reduced (●) and *S*-nitrosated (○) GSTP1-1 over time for representative peptides. Lines through the points are guides for the eye only. The plots are scaled according to the maximal number of exchangeable amide hydrogens for that peptide, assumed to equal the number of non-proline residues in the peptide minus the first two residues, which are subject to rapid back exchange.

quenching behavior (Figure 1). Cys47 does not participate directly in catalysis,[40] but chemical modification of the thiol impairs the activity of the enzyme.[41−43] Our DXMS data suggest that *S*-nitrosation at this residue inactivates GSTP1-1 by substantially increasing the dynamics of the active site (Figures 5 and 6).

Equilibrium unfolding experiments showed, strikingly, that *S*-nitrosation significantly reduces the unfolding cooperativity of GSTP1-1 (Figure 2). This indicates that the modification decreases the difference in solvent accessible surface area between the native and denatured states.[36] Acrylamide quenching experiments in 8 M urea support this by suggesting that the denatured state of *S*-nitrosated GSTP1-1 retains significant residual structure. Furthermore, data for the unfolding kinetics show that *S*-nitrosated GSTP1-1 unfolds quickly (high $k_u^{H_2O}$) and via a low-energy transition state (low $m_u^{\ddagger}$) (Figure 4). Together, these data indicate that *S*-nitrosation at Cys47 and Cys101 smoothes the unfolding energy landscape of GSTP1-1.

Trp28 is the dominant fluorophore of GSTP1-1, contributing 70% of the fluorescence signal.[44] Unlike Trp38, which is solvent-exposed even in the native state because of its position on the highly dynamic α2, Trp28 is relatively solvent inaccessible in reduced GSTP1-1 (Figure 6). This is consistent with the cooperative transition observed when the unfolding of the reduced protein is probed by tryptophan fluorescence; as the protein unfolds, the buried Trp28 becomes solvent-exposed in a concerted manner. The very low unfolding cooperativity of *S*-nitrosated GSTP1-1 is explained by our DXMS experiments, which reveal that the local environment of Trp28 becomes less ordered and more solvent accessible upon *S*-nitrosation (Figures 5 and 6). *S*-Nitrosation appears to substantially destabilize domain 1 of GSTP1-1 (proximal to Trp28 and -38), resulting in a partially disordered state that unfolds with low kinetic and thermodynamic cooperativity.

In addition to destabilizing domain 1, *S*-nitrosation increases the conformational flexibility of parts of domain 2, which is particularly stable in reduced GSTP1-1 (Figures 5 and 6). This is most apparent at longer deuteration times (>30 s), indicating that the conformational transitions that expose the amide hydrogens in domain 2 are much slower than those associated with domain 1. The increased dynamics of domain 2 may alter the folding energy landscape of *S*-nitrosated GSTP1-1, potentially explaining the low refolding cooperativity of this domain (Figure 3).

S-Nitrosation at Cys47 is disfavored whenever the G-site of GSTP1-1 is occupied,[30] for example, by GSH, glutathione disulfide, or the dinitrosyl−diglutathionyl−iron complex.[45] In addition, Cys47-NO is highly susceptible to denitrosation by GSH.[30] These factors are consistent with the low level of

dx.doi.org/10.1021/bi401414c | *Biochemistry* 2013, 52, 9394−9402

Cys47-NO GSTP1-1 observed *in vivo* (3−55% depending on the concentration of the NO donor).[21] *S*-Nitrosation at Cys47 is therefore only likely to occur under conditions of oxidative stress, when GSH concentrations are low and NO donors (GSNO and CysNO) are more abundant.[20] Cys101-NO of GSTP1-1 is relatively kinetically resistant to denitrosation by GSH[30] and unusually persistent *in vivo*.[19] We therefore also analyzed the stability and unfolding of Cys101-NO GSTP1-1, prepared by saturating the protein with GSO_3^- prior to *S*-nitrosation with GSNO. GSO_3^- binds the G-site of GSTP1-1, biasing the closed state of $\alpha 2$[37] and preventing *S*-nitrosation of Cys47.[30] *S*-Nitrosation at Cys101 reduces the cooperativity of unfolding of domain 1 of GSTP1-1, although not to the same extent as the fully nitrosated protein (Figure 2). It also introduces a refolding defect in the same domain, preventing the full recovery of the native state (Figure 3). In contrast to *S*-nitrosation at both cysteines, Cys101 nitrosation stabilizes the protein kinetically (Figure 4). This kinetic stabilization may compensate *in vivo* for the apparent thermodynamic destabilization and refolding defect. Although *S*-nitrosation at Cys101 alone does not affect the enzymatic activity of GSTP1-1,[22] it may affect the ability of GSTP1-1 to inhibit c-jun N-terminal kinase[46] or bind peroxiredoxin.[47]

GSTP1-1 is tightly regulated by *S*-nitrosation. GSNO spontaneously and rapidly *S*-nitrosates Cys47 when $\alpha 2$ is in its open conformation,[30] thereby introducing local disorder, destabilizing domain 1, and smoothing the unfolding energy landscape. Cys101 is nitrosated more slowly but persists *in vivo*,[19,30] introducing a refolding defect but kinetically stabilizing GSTP1-1. This work elucidates the regulation of GSTP1-1 by *S*-nitrosation at a molecular level, contributing to a general understanding of how cysteine *S*-nitrosation controls protein stability and activity.

■ ASSOCIATED CONTENT

Ⓢ Supporting Information

DXMS deuteration difference heat map (Figure S1) and a complete set of DXMS peptide uptake plots (Figure S2). This material is available free of charge via the Internet at http://pubs.acs.org.

■ AUTHOR INFORMATION

Corresponding Author

*Protein Structure-Function Research Unit, School of Molecular and Cell Biology, University of the Witwatersrand, Johannesburg, South Africa. E-mail: heinrich.dirr@wits.ac.za. Telephone: (+27) 11 717 6352.

Funding

Supported by the University of the Witwatersrand, South African National Research Foundation Grant 68898, and the South African Research Chairs Initiative of the Department of Science and Technology and National Research Foundation Grant 64788.

Notes

The authors declare no competing financial interest.

■ ABBREVIATIONS

$\alpha 2$, helix 2 of glutathione transferase P1-1; DXMS, hydrogen−deuterium exchange mass spectrometry; GST, glutathione transferase; GSH, glutathione; GSNO, *S*-nitrosoglutathione; GSO_3^-, glutathione sulfonate; S-NO, *S*-nitrosothiol; PDB, Protein Data Bank.

■ REFERENCES

(1) Lee, T.-Y., Chen, Y.-J., Lu, C.-T., Ching, W.-C., Teng, Y.-C., Huang, H.-D., and Chen, Y.-J. (2012) dbSNO: A database of cysteine S-Nitrosylation. *Bioinformatics 2012*, 2293−2295.

(2) Hess, D. T., Matsumoto, A., Kim, S., Marshall, H. E., and Stamler, J. S. (2005) Protein S-nitrosylation: Purview and parameters. *Nat. Rev. Mol. Cell Biol. 6*, 150−166.

(3) Hess, D. T., and Stamler, J. S. (2011) Regulation by S-nitrosylation of Protein Posttranslational Modification. *J. Biol. Chem. 287*, 4411−4418.

(4) Foster, M. W., Hess, D. T., and Stamler, J. S. (2009) Protein S-nitrosylation in health and disease: A current perspective. *Trends Mol. Med. 15*, 391−404.

(5) Hausladen, A., Privalle, C. T., Keng, T., DeAngelo, J., and Stamler, J. S. (1996) Nitrosative stress: Activation of the transcription factor OxyR. *Cell 86*, 719−729.

(6) Rössig, L., Fichtlscherer, B., Breitschopf, K., Haendeler, J., Zeiher, A. M., Mülsch, A., and Dimmeler, S. (1999) Nitric oxide inhibits caspase-3 by S-nitrosation in vivo. *J. Biol. Chem. 274*, 6823−6826.

(7) Xu, L. (1998) Activation of the Cardiac Calcium Release Channel (Ryanodine Receptor) by Poly-S-Nitrosylation. *Science 279*, 234−237.

(8) Asada, K., Kurokawa, J., and Furukawa, T. (2009) Redox- and calmodulin-dependent S-nitrosylation of the KCNQ1 channel. *J. Biol. Chem. 284*, 6014−6020.

(9) Wolzt, M., MacAllister, R. J., Davis, D., Feelisch, M., Moncada, S., Vallance, P., and Hobbs, A. J. (1999) Biochemical characterization of S-nitrosohemoglobin. Mechanisms underlying synthesis, no release, and biological activity. *J. Biol. Chem. 274*, 28983−28990.

(10) Kim, S. O., Merchant, K., Nudelman, R., Beyer, W. F., Jr., Keng, T., DeAngelo, J., Hausladen, A., and Stamler, J. S. (2002) OxyR: A Molecular Code for Redox-Related Signaling. *Cell 109*, 383−396.

(11) Malik, M., Shukla, A., Amin, P., Niedelman, W., Lee, J., Jividen, K., Phang, J. M., Ding, J., Suh, K. S., Curmi, P. M. G., et al. (2010) S-Nitrosylation Regulates Nuclear Translocation of Chloride Intracellular Channel Protein CLIC4. *J. Biol. Chem. 285*, 23818−23828.

(12) Tada, Y., Spoel, S. H., Pajerowska-Mukhtar, K., Mou, Z., Song, J., Wang, C., Zuo, J., and Dong, X. (2008) Plant immunity requires conformational changes [corrected] of NPR1 via S-nitrosylation and thioredoxins. *Science 321*, 952−956.

(13) Schreiter, E. R., Rodr1, M., Weichsel, A., Montfort, W. R., and Bonaventura, J. (2007) S-Nitrosylation-induced Conformational Change in Blackfin Tuna Myoglobin. *J. Biol. Chem. 282*, 19773−19780.

(14) Weichsel, A., Brailey, J. L., and Montfort, W. R. (2007) Buried S-nitrosocysteine revealed in crystal structures of human thioredoxin. *Biochemistry 46*, 1219−1227.

(15) Chen, Y. Y., Chu, H. M., Pan, K. T., Teng, C., Wang, D. L., Wang, A. H. J., Khoo, K. H., and Meng, T. C. (2008) Cysteine S-nitrosylation protects protein-tyrosine phosphatase 1B against oxidation-induced permanent inactivation. *J. Biol. Chem. 283*, 35265−35272.

(16) Weichsel, A., Maes, E. M., Andersen, J. F., Valenzuela, J. G., Shokhireva, T. K., Walker, F. A., and Montfort, W. R. (2005) Heme-assisted S-nitrosation of a proximal thiolate in a nitric oxide transport protein. *Proc. Natl. Acad. Sci. U.S.A. 102*, 594−599.

(17) Williams, J., and Pappu, K. (2003) Structural and biochemical studies of p21Ras S-nitrosylation and nitric oxide-mediated guanine nucleotide exchange. *Proc. Natl. Acad. Sci. U.S.A. 100*, 6376−6381.

(18) Lenarcic Zivkovic, M., Zareba-Koziol, M., Zhukova, L., Poznanski, J., Zhukov, I., and Wyslouch-Cieszynska, A. (2012) Post-translational S-Nitrosylation Is an Endogenous Factor Fine Tuning the Properties of Human S100A1 Protein. *J. Biol. Chem. 287*, 40457−40470.

(19) Paige, J. S., Xu, G., Stancevic, B., and Jaffrey, S. R. (2008) Nitrosothiol reactivity profiling identifies S-nitrosylated proteins with unexpected stability. *Chem. Biol. 15*, 1307−1316.

(20) Beltrán, B., Orsi, A., Clementi, E., and Moncada, S. (2000) Oxidative stress and S-nitrosylation of proteins in cells. *Br. J. Pharmacol. 129*, 953−960.

(21) Sinha, V., Wijewickrama, G. T., Chandrasena, R. E. P., Xu, H., Edirisinghe, P. D., Schiefer, I. T., and Thatcher, G. R. J. (2010) Proteomic and mass spectroscopic quantitation of protein S-nitrosation differentiates NO-donors. *ACS Chem. Biol. 5*, 667−680.
(22) Lo Bello, M., Nuccetelli, M., Caccuri, A. M., Stella, L., Parker, M. W., Rossjohn, J., McKinstry, W. J., Mozzi, A. F., Federici, G., Polizio, F., Pedersen, J. Z., and Ricci, G. (2001) Human glutathione transferase P1-1 and nitric oxide carriers; a new role for an old enzyme. *J. Biol. Chem. 276*, 42138−42145.
(23) Chang, M., Bolton, J. L., and Blond, S. Y. (1999) Expression and purification of hexahistidine-tagged human glutathione S-transferase P1-1 in *Escherichia coli*. *Protein Expression Purif. 17*, 443−448.
(24) Habig, W., and Jakoby, W. (1981) Assays for differentiation of glutathione S-transferases. *Methods Enzymol. 77*, 398−405.
(25) Lehrer, S. S. (1971) Solute perturbation of protein fluorescence. The quenching of the tryptophyl fluorescence of model compounds and of lysozyme by iodide ion. *Biochemistry 10*, 3254−3263.
(26) Eftink, M. R., and Ghiron, C. A. (1976) Exposure of tryptophanyl residues in proteins. Quantitative determination by fluorescence quenching studies. *Biochemistry 15*, 672−680.
(27) Zhang, H., Mcloughlin, S. M., Frausto, S. D., Tang, H., Mark, R., and Marshall, A. G. (2010) Simultaneous Reduction and Digestion of Proteins with Disulfide Bonds for Hydrogen/Deuterium Exchange Monitored by Mass Spectrometry. *Anal. Chem. 82*, 1450−1454.
(28) Téllez-Sanz, R., Cesareo, E., Nuccetelli, M., Aguilera, A. M., Barón, C., Parker, L. J., Adams, J. J., Morton, C. J., Lo Bello, M., Parker, M. W., et al. (2006) Calorimetric and structural studies of the nitric oxide carrier S-nitrosoglutathione bound to human glutathione transferase P1-1. *Protein Sci. 15*, 1093−1105.
(29) Liu, L., Hausladen, A., Zeng, M., Que, L., Heitman, J., and Stamler, J. S. (2001) A metabolic enzyme for S-nitrosothiol conserved from bacteria to humans. *Nature 410*, 490−494.
(30) Balchin, D., Wallace, L., and Dirr, H. W. (2013) S-Nitrosation of Glutathione Transferase P1-1 Is Controlled by the Conformation of a Dynamic Active Site Helix. *J. Biol. Chem. 288*, 14973−14984.
(31) Lo Bello, M., Parker, M. W., Desideri, A., Polticelli, F., Falconi, M., Del Boccio, G., Pennelli, A., Federici, G., and Ricci, G. (1993) Peculiar Spectroscopic and Kinetic Properties of Cys-47 in human placental glutathione transferase. *J. Biol. Chem. 268*, 19033−19038.
(32) Chen, X., Wen, Z., Xian, M., Wang, K., Ramachandran, N., Tang, X., Schlegel, H. B., Mutus, B., and Wang, P. G. (2001) Fluorophore-labeled S-nitrosothiols. *J. Org. Chem. 66*, 6064−6073.
(33) Bico, P., Erhardt, J., Kaplan, W., and Dirr, H. (1995) Porcine class pi glutathione S-transferase: Anionic ligand binding and conformational analysis. *Biochim. Biophys. Acta 1247*, 225−230.
(34) Dirr, H., and Reinemer, P. (1991) Equilibrium unfolding of class glutathione S-transferase. *Biochem. Biophys. Res. Commun. 180*, 294−300.
(35) Gildenhuys, S., Wallace, L. A., Burke, J. P., Balchin, D., Sayed, Y., and Dirr, H. W. (2010) Class pi glutathione transferase unfolds via a dimeric and not monomeric intermediate: Functional implications for an unstable monomer. *Biochemistry 49*, 5074−5081.
(36) Myers, J. K. K., Pace, C. N. N., and Scholtz, J. M. M. (1995) Denaturant m values and heat capacity changes: Relation to changes in accessible surface areas of protein unfolding. *Protein Sci. 4*, 2138−2148.
(37) Hitchens, T. K., Mannervik, B., and Gordon, S. (2001) Disorder-to-order transition of the active site of human class pi glutathione transferase, GST P1-1. *Biochemistry 40*, 11660−11669.
(38) Thompson, L. C., Walters, J., Burke, J., Parsons, J. F., Armstrong, R. N., and Dirr, H. W. (2006) Double mutation at the subunit interface of glutathione transferase rGSTM1-1 results in a stable, folded monomer. *Biochemistry 45*, 2267−2273.
(39) Stoychev, S. H., Nathaniel, C., Fanucchi, S., Brock, M., Li, S., Asmus, K., Woods, V. L., and Dirr, H. W. (2009) Structural dynamics of soluble chloride intracellular channel protein CLIC1 examined by amide hydrogen-deuterium exchange mass spectrometry. *Biochemistry 48*, 8413−8421.
(40) Kong, K.-H., Inoue, H., and Takahashi, K. (1991) Non-essentiality of cysteine and histidine residues for the activity of human class pi glutathione S-transferase. *Biochem. Biophys. Res. Commun. 181*, 748−755.
(41) Townsend, D. M., Manevich, Y., He, L., Hutchens, S., Pazoles, C. J., and Tew, K. D. (2009) Novel role for glutathione S-transferase pi. Regulator of protein S-glutathionylation following oxidative and nitrosative stress. *J. Biol. Chem. 284*, 436−445.
(42) Caccuri, A. M., Petruzzelli, R., Polizio, F., Federici, G., and Desiderittl, A. (1992) Inhibition of Glutathione Transferase 7r from Human Placenta by 1-Chloro-2,4-dinitrobenzene Occurs Because of Covalent Reaction with Cysteine 47. *Arch. Biochem. Biophys. 297*, 119−122.
(43) Sluis-cremer, N., and Dirr, H. (1995) Conformational stability of Cys45-alkylated and hydrogen peroxide-oxidised glutathione S-transferase. *FEBS Lett. 371*, 94−98.
(44) Stella, L., Caccuri, A., Rosato, N., Nicotra, M., Lo Bello, M., De Matteis, F., Mazzetti, A. P., Federici, G., and Ricci, G. (1998) Flexibility of helix 2 in the human glutathione transferase P1-1. *J. Biol. Chem. 273*, 23267−23273.
(45) De Maria, F., Pedersen, J. Z., Caccuri, A. M., Antonini, G., Turella, P., Stella, L., Lo Bello, M., Federici, G., and Ricci, G. (2003) The specific interaction of dinitrosyl-diglutathionyl-iron complex, a natural NO carrier, with the glutathione transferase superfamily: Suggestion for an evolutionary pressure in the direction of the storage of nitric oxide. *J. Biol. Chem. 278*, 42283−42293.
(46) Adler, V., Yin, Z., Fuchs, S. Y., Benezra, M., Rosario, L., Tew, K. D., Pincus, M. R., Sardana, M., Henderson, C. J., Wolf, C. R., Davis, R. J., and Ronai, Z. (1999) Regulation of JNK signaling by GSTp. *EMBO J. 18*, 1321−1334.
(47) Ralat, L. A., Misquitta, S. A., Manevich, Y., Fisher, A. B., and Colman, R. F. (2008) Characterization of the complex of glutathione S-transferase pi and 1-cysteine peroxiredoxin. *Arch. Biochem. Biophys. 474*, 109−118.